APPLIED PHYSICS LETTERS 110, 092103 (2017)

Solid solution strengthening in GaSb/GaAs: A mode to reduce the TD density through Be-doping

M. Gutiérrez,[1] D. Araujo,[1] P. Jurczak,[2] J. Wu,[2] and H. Liu[2]
[1]*Department of Material Science and Metallurgic Engineering, University of Cadiz, Puerto Real 11510, Spain*
[2]*Department of Electronic and Electrical Engineering, University College London, London WC1E 7JE, United Kingdom*

(Received 7 November 2016; accepted 7 February 2017; published online 1 March 2017)

The need for a low bandgap semiconductor on a GaAs substrate for thermophotovoltaic applications has motivated research on GaSb alloys, in particular, the control of plastic relaxation of its active layer. Although interfacial misfit arrays offer a possibility of growing strain-free GaSb-based devices on GaAs substrates, a high density of threading dislocations is normally observed. Here, we present the effects of the combined influence of Be dopants and low growth temperature on the threading dislocation density observed by Transmission Electron Microscopy. The Be-related hardening mechanism, occurring at island coalescence, is shown to prevent dislocations to glide and hence reduce the threading dislocation density in these structures. The threading density in the doped GaSb layers reaches the values of seven times less than those observed in undoped samples, which confirms the proposed Be-related hardening mechanism. [http://dx.doi.org/10.1063/1.4977489]

The commercially manufactured photovoltaic systems usually have low efficiencies, converting only about 10% of the incident radiation. Moreover, the semiconductor materials used to fabricate solar cells are expensive, which adds up to the overall high cost of photovoltaic electricity. For this energy source to become competitive, the price of photovoltaic solar energy should decrease to 0.1–0.25 €/kWh. To achieve this, it is essential to drastically increase the conversion efficiency from solar radiation to electricity. Harvesting low energy radiation as well, using thermophotovoltaic (TPV) cells, can significantly increase competitiveness of photovoltaics as the total conversion efficiency of solar-TPV systems could reach 30%. In these devices, the radiation from an emitter at about 1000–1500 °C (1.6–2.3 μm) is collected by a low band gap semiconductor cell. GaSb is of great interest as a potential cell material because it is a III–V semiconductor with a direct band gap of 0.72 eV at 300 °K and spectral response up to 1.75 μm. There have been attempts to transfer GaSb-based devices onto GaAs substrates; however, the lattice mismatch between GaSb and GaAs (7.8%) sets the critical layer thickness at 10 Å.

In the last decades, the use of a highly periodic array of perfect edge misfit dislocations (90° MDs), called interfacial misfit (IMF) array, has been reported as an effective method to create semicoherent interfaces in large lattice mismatch systems like GaSb-based devices on GaAs substrates.[1–6] Although it could be expected to obtain only the 90° MDs due to their energetically favourable state with respect to the 60° ones, both types are usually observed in this system at similar growth conditions.[7–9] The 60° MDs generate threading dislocations (TDs), which emerging from the interface glide to the surface resulting in material degradation, decrementing its electrical and optical properties.[10,11] Understanding the mechanism that determines defect type and density at the GaSb/GaAs interface depending on growth conditions is crucial since 90° MDs can completely relax the system, without formation of any TDs, whereas the 60° MDs can glide or interact with 90° MDs causing them also to glide further deteriorating the device performance by creation of more TDs.

It is well known that the growth temperature has a high impact on the type of MDs in GaSb grown on GaAs (001);[1,12] specifically, 90° MDs are observed at low growth temperatures (≈520 °C), while 60° ones appear at high temperatures (≈560 °C). Moreover, it was reported that dopants may effectively reduce the difference in surface mobility of group III elements along [110] and [1$\bar{1}$0] directions before stacking at an atomic location through an impurity-induced layer disordering intermixing effect.[13] These dopants should not contribute to parasitic parallel conduction since they are deactivated through compensation by high-density dislocations and defects (vacancies and antisites).[14,15] In this work, we propose the use of low growth temperature, specifically 510 °C, and beryllium dopants to enhance the crystal quality of GaSb-based materials grown on GaAs. The temperature chosen is high enough to obtain 2×8 surface reconstruction indicative of the single monolayer of Sb before the GaSb growth,[16] which has been observed to favour IMF formation.[5] Be is expected to act as a surfactant compensating the strain with Sb_{Ga} defects and improving the surface morphology.[17,18] Here, a Be-related hardening mechanism is proposed to attenuate the misfit dislocation glide and interaction and thus the generation of TDs.

Undoped GaSb and Be-doped GaSb (GaSb:Be) layers, samples A, B, and C, were grown on GaAs (001) by molecular beam epitaxy (MBE). In both n-type epi-ready GaAs (001), wafers were used as substrates. After desorption of an oxide layer at the substrate surface by annealing at 600 °C for 10 min, a 200 nm thick GaAs buffer layer was grown at 590 °C. As flux was stopped in 20 s, Sb flux was immediately supplied and the RHEED pattern has changed from 2×4 to

2×8. The growth temperature was then reduced from 590 to 510 °C to grow a 150-nm-thick undoped GaSb layer for sample A and Be doped to 5×10^{18} and 1×10^{19} cm^{-3} GaSb layer for samples B and C, respectively. Samples were studied using cross-section transmission electron microscopy (TEM). The TEM specimens were prepared using mechanical polishing techniques, followed by Ar^{+} ion sputtering at liquid-nitrogen temperature. TEM observations were carried out on a Philips CM 200 and a JEOL 2100 EX TEM operated at 200 keV.

The (001) GaSb/GaAs interface of sample A (undoped sample) was studied using 220 BF TEM and high-resolution transmission electron microscopy (HRTEM) taken in a [110] projection. The 220 BF TEM micrographs showed a highly periodic array of bright/dark spots localized at the GaSb/GaAs interface plane, which correspond to MD sites.[19] Careful examination of the atomic lattice surrounding the misfits using HRTEM (Fig. 1(a)) allowed the identification of an array of perfect edge MDs along the [110] direction resulting in a semicoherent interface, i.e., 90° MD type with Burgers vector of $a/2[1\bar{1}0]$ lying along the GaSb/GaAs interface and two extra {111} planes symmetrically located at the dislocation core. The MD separation was determined to be around 5.7 nm, which corresponds to 13 GaSb lattice sites and 14 GaAs lattice sites.[2] Thus, every 14th Ga atom had a pair of dangling bonds to accommodate the larger Sb atom in the next (001) plane. Note that in sample A, all these MDs are located in the same (001) interface plane and an identical misfit array was also observed in the GaSb/GaAs interface along the perpendicular [110] direction.

The selected area electron diffraction (SAED) pattern at the GaSb/GaAs interface of sample A is shown in the inset of Fig. 1(a). These diffraction patterns (DPs) were used to estimate strain relief generated by the lattice mismatch. The calculation of the GaSb lattice parameter based on the diffraction spots of GaAs as the bulk material (5.65 Å) determined that 98% of the strain energy of the GaSb layer was dissipated by the MD array at the GaSb/GaAs interface.

The HRTEM studies revealed that the behaviour of dislocations in GaSb:Be/GaAs, samples B and C (Be-doped samples), is different from that in sample A, i.e., two types of areas at the interface were observed in this sample. On one hand, there were areas with similar configuration to that of sample A where 90° MDs were sited at the GaSb:Be/GaAs interface plane, see Fig. 1(b), while, on the other hand, there were also areas with 60° MDs not located at the interface plane. Fig. 1(c) is an example of these latter areas; dashed yellow lines point out some 60° MDs and yellow circles point out zones where it is impossible to draw the dislocations with precision.

To complete the study, SAED patterns were recorded at the interface (Fig. 1 insets). As it can be observed, the DP of Fig. 1(b), as in Fig. 1(a), shows no coincidence of GaAs and GaSb spots, which allowed calculation of relaxation of the GaSb layer as also 98%. However, the spot pointed with the white arrow in Fig. 1(c), corresponding to the [100] direction

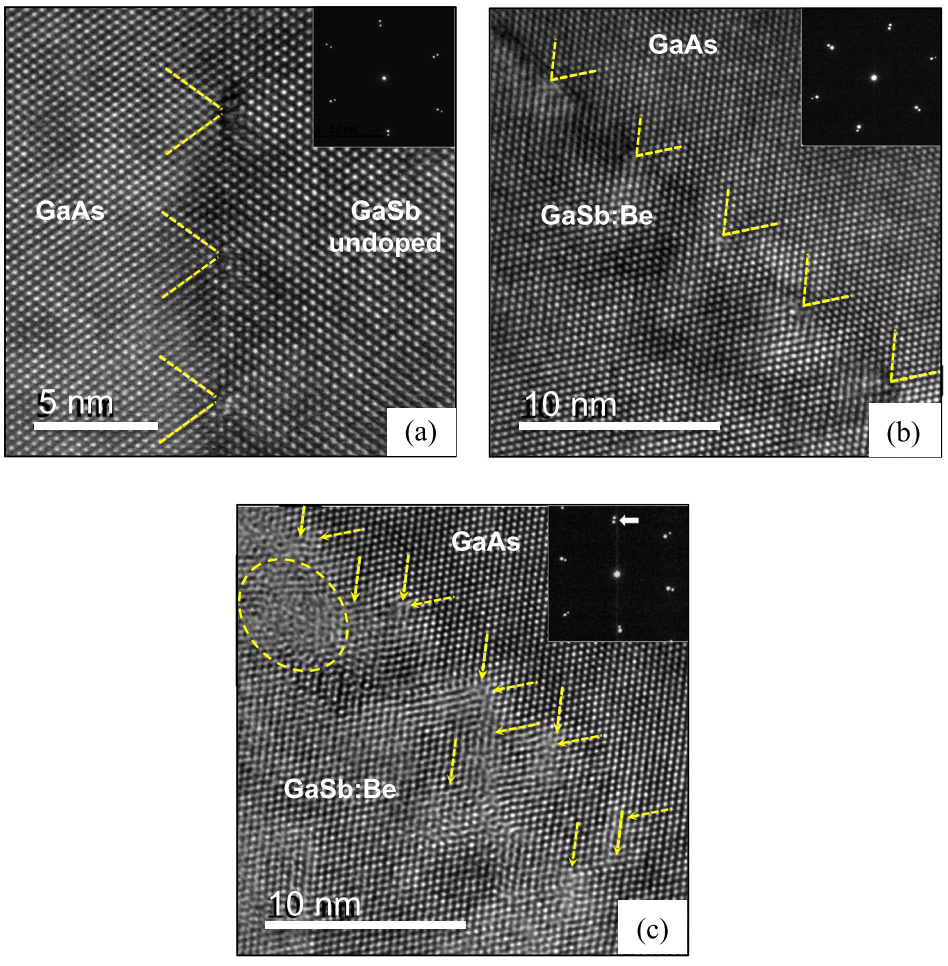

FIG. 1. HRTEM micrographs and their corresponding DP of (a) the IMF dislocation array throughout the GaSb/GaAs interface of sample A, (b) an area of sample B analogous to sample A, and (c) an area of sample B where some of the 60° MDs are located.

of the GaSb:Be layer, is turned 2° about the [100] direction of the GaAs substrate. This tilt has been explained by Kang *et al.*:[20] asymmetric distribution of 60° MDs at the interface is more energetically favourable than the symmetric one because the first one produces accumulation of their vertical edge component. Thus, in sample A (GaSb/GaAs) along both ⟨110⟩ directions dislocations are shown to lie only at the interface, while in sample B (GaSb:Be/GaAs) intervals of approximately 200 nm length with 90° MDs are separated by other intervals of approximately 30 nm length where 60° MDs are located outside the GaSb/GaAs interface plane up to 20 nm away. This different dislocation configuration is attributed to the following GaSb growth mechanism (see Fig. 2).

Step 1: The initial steps of GaSb growth on (001) GaAs substrates by MBE correspond to the Volmer-Weber growth model.[5] Islands are formed to relax the tetragonal distortion due to the very large lattice mismatch (7.8%). These islands are flat-topped, have uniform height, and are bound by {111} planes.[1] The initial strain relief of this highly mismatched island is governed by an IMF array of pure edge 90° MDs along [110] and [1$\bar{1}$0] directions located at the GaSb/GaAs interface. Qian *et al.*[21] proposed that 90° MDs at the GaSb/GaAs (001) interface nucleate at the leading edges of advancing {111} planes and glide inward (001) interface during island growth to reach the equilibrium position. Moreover, they do not generate threading dislocations (TDs) inside the islands due to their sessile nature in {111} planes, as shown in Fig. 2(a).

Step 2: The IMF array is an energetically favourable state, since 90° MDs are twice as efficient as the 60° ones for strain relaxation, but requires balancing of strain energy with adatom migration function of growth parameters. As more GaSb is deposited, the islands reach a critical height where the strain can be partly relieved by bending of the atomic planes to the free surface under the leading edges. This configuration results in nucleation of 60° MDs[22] at the leading edges as indicated in Fig. 2(b).

Step 3: When more than the nominal 80 nm of GaSb is deposited, the islands are wide enough to coalesce. At this point, the 60° MDs of each leading edge interact with the previously formed 90° MDs to generate TDs.[20]

When the coalescence areas reach upper parts of the islands, new 60° MDs are formed at the coalescence zones, followed by one of these two processes:

(1) Figure 2(c)–step 3.1 and Figure 2(d)-step 4.1: These new 60° MDs, nucleated where the circles of the Fig. 2(c)–step 3.1 are, glide down to the GaSb/GaAs interface along {111} planes where interactions with the 90° MD array (Fig. 2(d)-step 4.1) produce more TDs that propagate from the interface plane to the top surface. This process occurs in sample A, resulting in a TD density of $6.7 \times 10^{-4}\,\mathrm{nm}^{-2}$.
(2) Figure 2(c)–step 3.2 and Figure 2(d)-step 4.2: The presence of Be hardens the GaSb alloy by solid solution, i.e., limits the dislocation mobility. 60° MDs, formed on coalescence zones of sample B, are pinned by the lattice distortions produced by the Be dopants. In this situation, the dislocations cannot glide down to the GaSb/GaAs interface pushed by the GaSb layer lattice strain and their interaction with the 90° MD is avoided.

TDs density is usually given in terms of nm^{-1}, which is highly dependent on the area where the TEM micrograph is taken, i.e., micrographs taken with the same magnification but in areas of different thicknesses would imply different TD densities. Besides, a low magnification TEM micrograph will look like with different density areas if the sample thickness changes along the micrograph. Obviously, the TD density does not change with thickness; thus, here the TD density is expressed in terms of the number of TDs emerging from the GaSb/GaAs interface per its area. In Fig. 3(a),

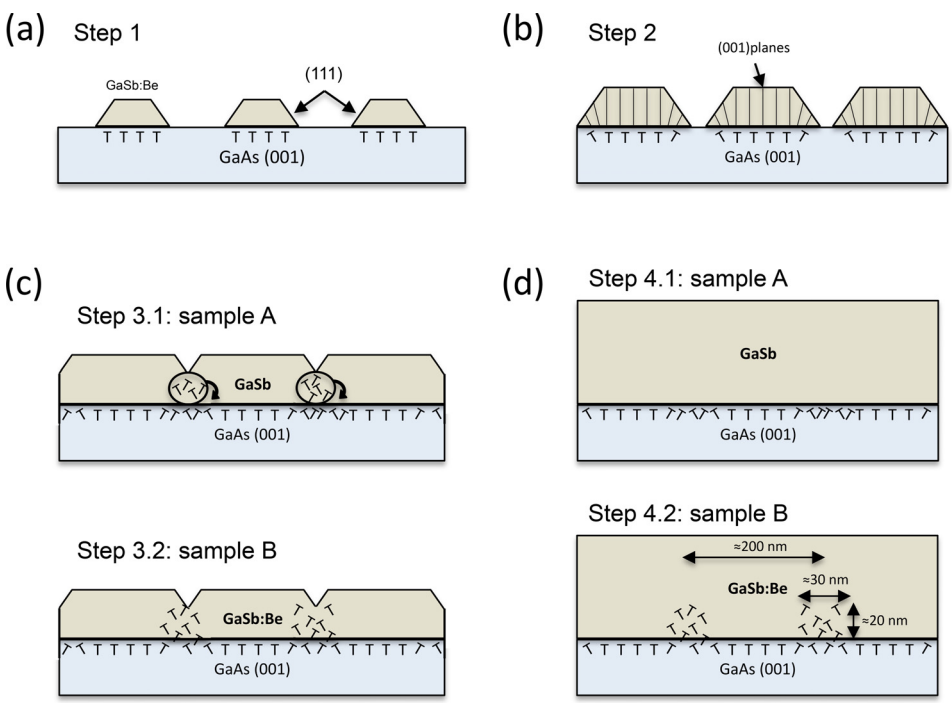

FIG. 2. Schematic representation of MD formation and distribution on the GaSb:Be/GaAs heterostructure. (a) Step 1: initial islands following the Volmer-Weber growth model. (b) Step 2: Strain relaxation by IMF network (⊤) and 60° MDs at the leading edges (⩛). (c) Step 3: Distribution of the 60° MDs originated in the coalescence areas for both samples. (d) Step 4: Final distribution of 90° and 60° MDs at the GaSb:Be/GaAs system.

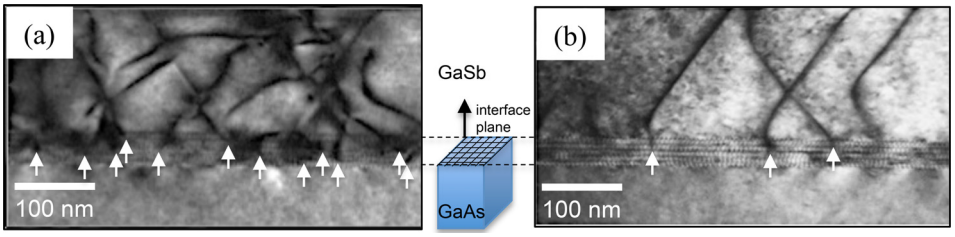

FIG. 3. Cross-sectional 220 BF TEM micrographs at the interface of (a) GaSb/GaAs (sample A) and (b) GaSb:Be/GaAs (sample B). Both micrographs, taken with the same sample thickness, magnification and angle, make evident the influence of Be dopant in the TD density. The (001) plane at the GaSb/GaAs interface is schematically shown in the middle of both micrographs to help in understanding the MD configuration. White arrows indicate the TD generation locations.

it can be observed that 12 TDs (indicated with white arrows) emerge out from an interface 517.6 nm wide and 34.2 nm deep. The first number is the width of the micrograph and the second one is the sample thickness, which was estimated from the facts that: (a) 90° MDs form a square array whose spacing in both ⟨110⟩ directions is 5.7 nm and (b) the contrasts due to MD lines perpendicular to the {110} plane look like black/white circles. When the sample is tilted to get 220 BF TEM conditions, these contrasts look elongated (lines) and are broken by MD lines parallel to the {110} plane (see Fig. 3). Counting the contrast breaks of one MD line perpendicular to the plane of the micrograph, the number of MDs perpendicular to this one is established. Since the distance between these MDs or breaks is exactly 5.7 nm, the sample thickness can be estimated. Thus, the GaSb/GaAs interface extension in Fig. 3 corresponds to a surface of 517.6 nm $\times$ 34.2 nm $=$ 17 701.92 nm^2, where 12 TDs are shown to be generated at this interface in the undoped sample (A) and 3 TDs in the Be-doped one (B). This leads to a surface TD density generation of $12/17\,701.92 = 6.7 \times 10^{-4}$ nm^{-2} and $3/17\,701.92 = 2.3 \times 10^{-4}$ nm^{-2}, respectively (almost three times less). Similar behaviour has been observed in the sample with a Be-doping concentration of 1×10^{19} cm^{-3} (sample C), which gave place to a TD density of 9.5×10^{-5} nm^{-2}. In this case, the TD density has a very significant improvement since it is reduced seven times.

It is remarkable that the sample preparation used for this study allows having 1 mm long electron-transparent areas so the micrographs shown in this paper are some of the tens that have been obtained.

Step 4: Higher thicknesses than the nominal 80 nm of GaSb on GaAs result in a two-dimensional growth where 60° dislocations can easily glide to the surface, which deteriorates device performance. Since solid solution hardening occurs in samples B and C, the TD generation during the two-dimensional growth is significantly reduced to 2.3×10^{-4} and 9.5×10^{-5} nm^{-2}, as mentioned before.

In conclusion, the use of low temperature and Be dopants can effectively reduce the TD density in GaSb layers grown on GaAs. In the coalescence areas between the GaSb islands, 60° MDs are nucleated and due to the large mismatch they glide down to the GaSb/GaAs interface plane to relieve the system stress. However, these 60° MDs also interact with the IMF dislocation array leading to formation of the undesirable TDs. Be dopants have been demonstrated to pin the 60° MDs at the island coalescence areas, hence reducing seven times the TD generation via solid solution hardening mechanism.

The authors cordially thank F. M. Varela of the University of Seville for co-operation during the use of the Philips CM 200 microscope placed at CITIUS centre.

This work has been supported by Spanish Ministry of Economy and Competitiveness (Ref.: TEC2014-54357-C2-2-R, HiVolt-nano project).

[1]S. H. Huang, G. Balakrishnan, A. Khoshakhlagh, A. Jallipalli, L. R. Dawson, and D. L. Huffaker, Appl. Phys. Lett. **88**, 131911 (2006).
[2]S. Huang, G. Balakrishnan, and D. L. Huffaker, J. Appl. Phys. **105**, 103104 (2009).
[3]A. Jallipalli, G. Balakrishnan, S. H. Huang, T. J. Rotter, K. Nunna, B. L. Liang, L. R. Dawson, and D. L. Liang, Nanoscale Res Lett. **4**, 1458 (2009).
[4]W. Zhou, X. Li, S. Xia, J. Yang, W. Tang, and K. M. Lau, J. Mater. Sci. Technol. **28**, 132 (2012).
[5]K. H. Tan, B. W. Jia, W. K. Loke, S. Wicaksono, and S. F. Yoon, J. Cryst. Growth **427**, 80 (2015).
[6]B. C. Juang, R. B. Laghumavarapu, B. J. Foggo, P. J. Simmonds, A. Lin, B. Liang, and D. L. Huffaker, Appl. Phys. Lett. **106**, 111101 (2015).
[7]P. E. Hopkins, J. C. Duda, S. P. Clark, C. P. Hains, T. J. Rotter, L. M. Phinney, and G. Balakrishnan, Appl. Phys. Lett. **98**, 161913 (2011).
[8]Y. Wang, P. Ruterana, L. Desplanque, S. El Kazzi, and X. Wallart, J. Appl. Phys. **109**, 023509 (2011).
[9]Y. Wang, P. Ruterana, S. Kret, S. El Kazzi, L. Desplanque, and X. Wallart, Appl. Phys. Lett. **102**, 052102 (2013).
[10]Q. Dai, M. F. Schubert, M. H. Kim, J. K. Kim, E. F. Schubert, D. D. Koleske, M. H. Crawford, S. R. Lee, A. J. Fischer, G. Thaler, and M. A. Banas, Appl. Phys. Lett. **94**, 111109 (2009).
[11]D. Cherns, S. J. Henley, and F. A. Ponce, Appl. Phys. Lett. **78**, 2691 (2001).
[12]J. H. Kim, T. Y. Seong, N. J. Mason, and P. J. Walker, J. Electron. Mater. **27**, 466 (1998).
[13]F. A. Kish, W. E. Plano, K. C. Hsieh, A. R. Sugg, N. Holonyak, Jr., and J. E. Baker, J. Appl. Phys. **66**, 5821 (1989).
[14]M. Haiml, U. Siegner, F. Morier-Genound, and U. Keller, Appl. Phys. Lett. **74**, 1269 (1999).
[15]J. K. Sheu and G. C. Chi, J. Phys.: Condens. Matter **14**, R657 (2002).
[16]L. J. Whitman, B. R. Bennett, E. M. Kneedler, B. T. Jonker, and B. V. Shanabrook, Surf. Sci. **436**, L707 (1999).
[17]S. J. Jo, S. G. Ihn, J. I. Song, J. G. Park, and D. H. Lee, Jpn. J. Appl. Phys. **45**, 724 (2006).
[18]H. P. Komsa, W. Arola, J. Pakarinen, C. S. Peng, and T. T. Rantala, Phys. Rev. B **79**, 115208 (2009).
[19]D. B. Williams and C. B. Carter, *Transmission Electron Microscopy* (Kluwer Academic/Plenum, New York, 1996).
[20]J. M. Kang, M. Nouaoura, L. Lassabatére, and A. Rocher, J. Cryst. Growth **143**, 115 (1994).
[21]W. Qian, M. Skowronski, R. Kaspi, M. De Graef, and V. P. Dravid, J. Appl. Phys. **81**, 7268 (1997).
[22]L. Vescan, W. Jäger, C. Dieker, K. Schmidt, A. Hartmann, and H. Lüth, Mater. Res. Soc. Symp. **263**, 23 (1992).